Contrib Mineral Petrol (1995) 121:424–436

F. P. Florence · R. S. Darling · S. E. Orrell

Moderate pressure metamorphism and anatexis due to anorthosite intrusion, western Adirondack Highlands, New York

Received: 13 September 1994 / Accepted: 10 May 1995

Abstract Garnet-sillimanite-biotite gneiss near Port Leyden, in the western Adirondack Highlands, New York, contains mineral assemblages and textures that formed during high temperature metamorphism and anatexis at mid-crustal pressures. Evidence for melting includes thin, plagioclase-rich veins, sieve textures in biotite, and the presence of small, euhedral garnet neoblasts. Hercynite-silicate equilibria in combination with the solidus for biotite dehydration melting indicate metamorphic pressure was between 4 and 6.4 kbar at the temperature of melting (ca. 735° C). The gneiss is intruded by a small, discordant Fe-Ti oxide-apatite (nelsonite) dike. Reported field occurrences of nelsonite demonstrate its common association with anorthosite plutons. Although no anorthosite bodies are exposed in the Port Leyden region, the presence of nelsonite is evidence of anorthositic magmatism in the western Adirondacks. Post-intrusion metamorphism has caused partial apatite recrystallization and produced a weak foliated texture in the dike. U-Pb ages from zircon and monazite from both the gneiss and the nelsonite dike indicate that these rocks experienced a complex, polymetamorphic history that we interpret to reflect two thermal episodes. An older event is recorded by discordant zircons in the gneiss, which indicate a minimum age of 1129±6 Ma. A linear best fit to the data yields an upper intercept at 1166±53 Ma. This range of ages coincides with anorthosite-suite magmatism in the Adirondacks. A minimum zircon age of 1104±3 Ma was obtained from the nelsonite dike. Lead-loss or late zircon crystallization at about 1020 Ma affected the U-Pb systematics of zircon in the dike. Monazite ages from both rocks also indicate high temperature metamorphism (>700° C) between 1040 and 960 Ma. The older zircon ages and textural relations in the metapelite are viewed as evidence for anatexis at ca. 1150 Ma, and the presence of nelsonite suggests that the intrusion of anorthosite was coincident with partial melting in the gneiss. *P-T* estimates of metamorphism, therefore, imply that anorthosite was emplaced to about 15 km depth in the western Adirondack Highlands.

F.P. Florence (✉) · S.E. Orrell
Department of Earth Sciences, Syracuse University, Syracuse, NY 13244, USA

R.S. Darling
Department of Geology SUNY College at Cortland, P.O. Box 2000, Cortland, NY 13045, USA

Editorial responsibility: K. Hodges

Introduction

The Adirondack Highlands, New York, form the southernmost exposed portion of the Central Granulite Terrane of the Precambrian Grenville Province (Wynne-Edwards 1972). Within this region of complexly folded orthogneiss and paragneiss are the large Marcy anorthosite massif and a number of smaller anorthosite bodies. Oxygen isotope study supports the emplacement of the Marcy anorthosite at shallow crustal depths. Valley and O'Neil (1982) measured low $\delta^{18}O$ in wollastonite skarns adjacent to the Marcy anorthosite and argued that this was the result of isotopic exchange with meteoric water, implying that contact metamorphism occurred in the upper 10 km of the crust. However, geobarometry estimates from Adirondack anorthosites and related orthogneiss indicate equilibration at crustal depths in excess of 23 km (Bohlen et al. 1985). These barometry estimates are based on mineral assemblages that commonly include garnet. As discussed by Bohlen et al. (1985), garnet growth in the orthogneisses likely represents metamorphism that post-dates anorthosite magmatism by more than 100 Ma. More precise estimation of the emplacement depths of these rocks has been hampered by the lack of suitable phase equilibria that can be shown to have developed synchronously with anorthosite intrusion.

We report here on the *P-T* conditions of mineral equilibria preserved in a high grade metapelitic gneiss in the western Highlands. This unit hosts a small Fe-Ti oxide + apatite dike that was comagmatic with the anorthosite intrusions in the Adirondack Highlands (Darling and

Florence 1995). U-Pb age data were obtained from zircon and monazite from the dike and the host gneiss in order (a) to determine the intrusion age of the dike and (b) to test the hypothesis that high grade metamorphism and partial melting in the Port Leyden region was the result of anorthosite suite magmatism associated with the intrusion of the nelsonite dike. Although we found complex U-Pb systematics in these minerals that resulted from a metamorphic episode post-dating the established ages for anorthosite magmatism, both rocks contain older zircons with similar minimum ages. Based on the presence of the nelsonite dike, the similarity in older zircon ages in the dike and the gneiss, and the coincidence of zircon fraction upper intercepts with the timing of anorthosite magmatism, we suggest that silicate and oxide mineral assemblages, formed in the gneiss during anatexis, provide useful geobarometry estimates for determining the emplacement depths of anorthosite suite rocks.

Thermotectonic setting

Recent geochronologic studies of intrusive and metamorphic rocks in the Adirondack Highlands (McLelland et al. 1988a; Mezger et al. 1991; Chiarenzelli and McLelland 1991) make it clear that multiple episodes of igneous activity and tectonism impacted this region during the Proterozoic. A profound episode of bimodal anorogenic plutonism occurred between 1157 and 1125 Ma. During this time, large anorthosite massifs and related mangerite, charnockite, and granite plutons, referred to as the AMCG suite (Emslie 1978; McLelland et al. 1988a), were intruded into calc-silicate and pelitic sedimentary rocks in the Highlands. The formation of wollastonite skarns in metasediments adjacent to AMCG plutons indicates that, at least locally, the intrusive episode was accompanied by high temperature metamorphism (Valley et al. 1990). Following cessation of AMCG magmatism, the Adirondack Highlands experienced metamorphism that coincided with the Ottawan phase of the Grenville orogeny (Moore and Thompson 1980). This metamorphic event produced U-Pb ages of between about 1050 and 1000 Ma in a suite of minerals, including zircon, garnet, monazite, and titanite (Mezger et al. 1991; Chiarenzelli and McLelland 1993). Bohlen et al. (1985) reported estimates of the pressures and temperatures of metamorphism based on mineral compositions that likely reflect conditions from this 1050–1000 Ma period. Their results indicate that pressures of 7 to 8 kbar were reached throughout the Highlands during granulite facies metamorphism.

The metamorphic grade and deformation that accompanied Ottawan metamorphism caused extensive recrystallization and compositional modification of minerals throughout much of the Adirondacks. AMCG intrusions commonly contain garnet, generally have metamorphic fabrics, and locally are folded (McLelland et al. 1988b). Chiarenzelli and McLelland (1993) described a pattern of increased lead loss and alteration of zircons from AMCG rocks that is correlated with a concentric trend of higher temperature geothermometry estimates in the central Highlands (Bohlen et al. 1985). Ottawan metamorphism was followed by a protracted period of cooling through mineral closure temperatures (Mezger et al. 1991), and retrograde exchange reactions plus diffusion can be expected to have eradicated much of the evidence of earlier thermal conditions (Spear and Florence 1992). Consequently, there have so far been no thermobarometric data from the Adirondacks that unambiguously fix the depths of anorthosite intrusion.

Mineral assemblages and textures

A 3 km-wide band of pelitic gneiss bounded by NE trending leucocratic gneiss, calc-silicate, and amphibolite is exposed in the vicinity of the town of Port Leyden in the western Adirondack Highlands (Fig. 1). The metapelite gneiss has an overall coarse-grained texture and typically contains the assemblage K-feldspar + biotite + plagioclase + sillimanite + garnet + quartz + ilmenite ± hercynite (Fe-spinel). For the most part it is a gray, granoblastic gneiss with foliation defined by aligned biotite and discontinuous mm to cm wide quartz-sillimanite-oxide segregations. There is sometimes a weak secondary foliation of biotite that intersects the dominant foliation at a high angle. However, within 0.5 km of the SE contact of the metapelitic zone, horizons within the gneiss display distinctive veining and mineral textures that we interpret to be the products of partial melting. Fine-grained granoblastic plagioclase, quartz, and prismatic sillimanite form thin (mm wide) leucocratic veins that cut across a coarse-grained matrix of perthitic K-feldspar. In these veins biotite, ilmenite, and garnet are surrounded by rims of plagioclase, quartz, and sillimanite. Rimmed biotite grains commonly have embayed and curved margins suggestive of resorption (Fig. 2A). These veined rocks also have sieve textured biotites scattered throughout the matrix.

Two textural varieties of garnet are recognized in samples with leucocratic veining. The most common garnets are porphyroblasts distributed throughout the matrix that range in size to 2 mm in diameter. Garnet porphyroblasts generally have irregular margins suggestive of resorption, although portions of grain margins commonly show a number of textural features indicating late growth. Sillimanite needles are present as inclusions in core regions of many of the garnets, but are absent from grain margins. Some

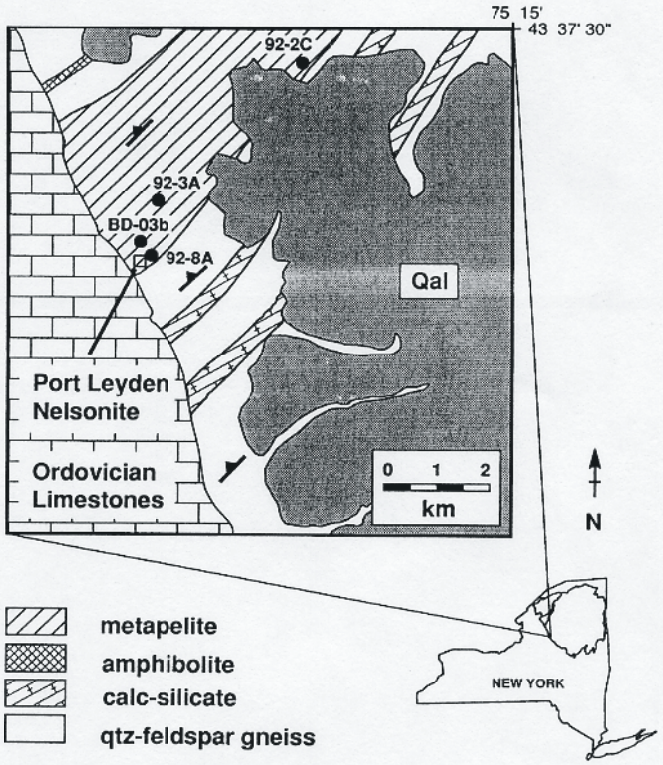

Fig. 1 Simplified geologic map of a portion of the Port Leyden quadrangle, New York, showing metamorphic lithologies, sample sites, and the location of the nelsonite intrusion. Regional foliation tends to parallel lithologic boundaries. Melt-related textures were observed in metapelitic gneiss within 0.5 km of the intrusion and in exposures of gneiss extending about 6 km to the northeast. *Qal* indicates Quaternary alluvium

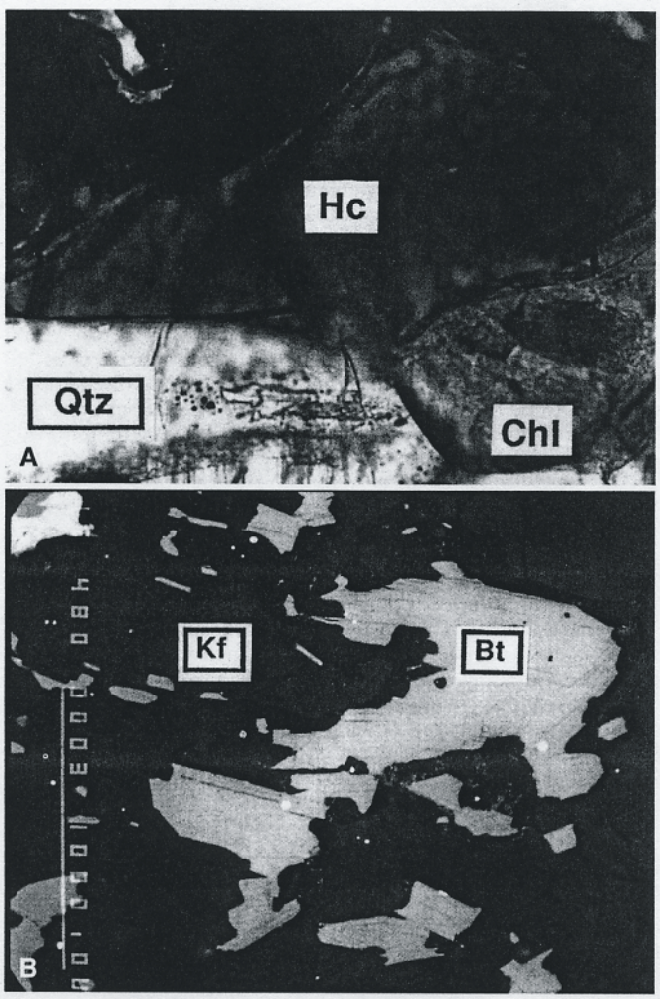

Fig. 2 **A** Photomicrograph showing sharp hercynite-quartz contact in sample BD-03b. The right side of the hercynite grain is adjacent to chlorite alteration. Width of photo 0.3 mm. **B** Electron micrograph showing melt textures around biotite in sample 92-2C2. Melt zone is now composed of quartz, plagioclase, and sillimanite. Note curved grain boundaries on biotite that parallel the contact of the melt zone with K-feldspar. Scale bar (left side) 1000 μm

garnets have one or more well-formed crystal faces and, less commonly, distinctly faceted inclusions of feldspar and quartz. Other textural features suggesting late growth include faceted garnet rims with embayments of quartz surrounded by K-feldspar and abundant inclusions of oxides in the outermost portions of the grains. The second garnet morphology is exhibited by relatively less abundant, small (ca. 200 μm diameter) inclusion-free garnets that are characteristically euhedral and commonly found in contact with biotite.

Dark green hercynite, although nowhere abundant, is present in many of the samples. It most commonly occurs adjacent to ilmenite, but also forms isolated grains. Ilmenite is present as disseminated grains in the matrix and is locally abundant in plagioclase-rich veins. Reaction textures are common in the oxides: ilmenite variably contains inclusions of hercynite and corundum, is partly replaced by rutile, and has hercynite, sillimanite, and garnet overgrowths on grain margins. Hercynite contains inclusions of corundum and a few of the hercynite grains are thinly rimmed with rutile. In a few samples hercynite is in direct contact with quartz (Fig. 2B) but more commonly there is a thin zone of sillimanite separating the two phases.

The mineral suite and mineral textures of the metapelites reflect two episodes of metamorphism. One involved biotite dehydration and garnet crystallization during partial melting. The distinctive textures of resorbed and sieve-textured biotite, plagioclase-quartz-sillimanite veining, and growth of euhedral garnet grains and crystal faces, are viewed as strong evidence for anatexis of these rocks (discussed in the following sections). Hercynite, corundum, and ilmenite are all present as inclusions in garnet rims, so their crystallization must have either preceded melting or was approximately coeval with it. These rocks have not undergone strong deformation since partial melting, but a few mineral textures indicate later metamorphism. Randomly oriented, idioblastic biotite grains and clots of biotite are scattered throughout the matrix. Rutile, which is nowhere found as an inclusion in garnet, is commonly associated with these biotites. Rutile also forms thin overgrowths on some hercynite grains and is sometimes observed partially replacing ilmenite.

Mineral chemistry

Compositional data for solid solution phases from the gneiss were obtained with a JEOL electron microprobe, and representative analyses are presented in Table 1. Operating conditions for the beam were 15 kV and 10–50 nA. Beam size was kept at a minimum (ca. 1–2 μm) for most analyses, but the diameter was expanded up to 25 μm for analysis of biotite and to assess the compositional homogeneity of spinel and plagioclase. Point analyses, line traverses, and two dimensional X-ray maps were used to measure compositions and compositional variations within individual grains of all minerals.

Garnets are almandine-rich, and in most samples contain only minor amounts of manganese and calcium. Sample BD-03b is distinctly richer in X_{Sps} and contains slightly lower X_{Grs}. None of the garnets appear to preserve growth zoning, but all of them have zoning profiles in the outermost 50 and 80 μm with outwardly increasing Fe and decreasing Mg (Fig. 3C). We interpret this compositional zoning as evidence of diffusion of Fe and Mg accompanying reequilibration during cooling. The presence of this zoning on the small euhedral grains and large grains with euhedral facets demonstrates that this cooling episode post-dates crystallization related to anatexis. Retrograde exchange of Fe and Mg between biotite and garnet is most pronounced where these minerals are in contact, but the presence of diffusionally induced zoning in all garnets implies that biotite compositions throughout the samples were likely modified by retrograde reaction.

Plagioclase composition is between An_{32} to An_{37} in most samples. Plagioclase in one sample (BD-03b) has albite rims on grain boundaries in contact with K-feldspar and patchy albitic domains surrounded by regions that were measured as An_{11} to An_{16} using a tightly focused microprobe beam. These compositional features suggest that peristeritic exsolution may have produced albite lamellae that are finer than can be resolved by the microprobe. Abundance of plagioclase increases sharply over a 10 cm wide zone in the contact zone adjacent to the dike, and plagioclase composition in individual grains within this zone varies from An_{36} to An_{42}. The relatively higher anorthite contents in this zone may have been the result of an increased local availability of calcium that was released during dissolution of apatite within the dike. Plagioclase composition from the thin veins outside of the contact zone varied substantially less. Plagioclase inclusions in K-feldspar and hercynite in sample 92–2C2 had slightly lower X_{An} relative to matrix grains (0.34 vs 0.36). Individual grains were homogeneous at the detection level of the electron microprobe.

Biotite compositions show variability over the scale of a thin section. Individual grains are homogeneous, but Fe/(Fe+Mg) values for any sample lie in a range between 0.45 and 0.52. TiO_2 for almost all biotites examined is between 4 and 5 wt%. The highest TiO_2 and Fe/(Fe+Mg) were measured in grains rimmed by plagioclase or K-feldspar, and lowest Fe/(Fe+Mg) is present in grains adjacent to garnet. Fluorine abundances in biotite more than 10 cm

Table 1 Mineral compositions in cations per mineral formula

Garnet	Cations per 12 oxygens					
Sample	92-2C2	92-2C4	92-2C6	92-3A	92-8A	BD-03b
Si	2.980	2.961	2.992	2.985	2.962	2.964
Al	1.999	2.024	1.979	2.008	2.018	2.045
Mg	0.500	0.596	0.569	0.558	0.499	0.336
Fe[a]	2.368	2.318	2.352	2.207	2.272	2.169
Mn	0.062	0.020	0.028	0.165	0.160	0.440
Ca	0.111	0.109	0.099	0.089	0.116	0.059
Oxide sum	100.67	100.57	100.74	101.39	101.17	100.47
$X_{grossular}$	3.65	3.58	3.25	2.95	3.81	1.96
Spinel	Cations per 4 oxygens					
Sample	92-2C2	92-2C4	92-2C6	92-3A	92-8A	BD-03b
Al	1.905	1.918	1.903	1.885	1.856	1.973
Ti	0.000	0.005	0.000	0.002	0.000	0.005
Mg	0.100	0.161	0.188	0.179	0.106	0.102
Fe[a]	1.008	0.894	0.920	0.680	0.879	0.725
Mn	0.002	0.000	0.002	0.005	0.009	0.022
Zn	0.028	0.058	0.035	0.129	0.055	0.182
Oxide sum	100.26	100.28	100.40	100.89	100.99	100.52
Plagioclase	Cations per 8 oxygens					
Sample	92-2C2	92-2C4	92-2C6	92-3A	92-8A	BD-03b
Si	2.610	2.689	2.662	2.718	2.579	2.855
Al	1.366	1.298	1.323	1.272	1.410	1.147
Fe[a]	0.005	0.001	0.007	0.120	0.002	0.000
Ca	0.393	0.328	0.351	0.262	0.404	0.150
K	0.008	0.011	0.007	0.007	0.009	0.011
Na	0.656	0.680	0.658	0.757	0.633	0.826
Oxide sum	99.97	99.08	100.02	100.36	99.45	99.40
A_N	37.5	32.5				15.4
Biotite	Cations per 11 oxygens					
Sample	92-2C2	92-2C4	92-2C6	92-3A	92-8A	BD-03b
Si	2.777	2.781	2.814	2.770	2.774	2.727
Al	1.340	1.392	1.325	1.413	1.426	1.466
Ti	0.263	0.224	0.252	0.164	0.159	0.280
Mg	1.232	1.327	1.352	1.357	1.269	1.230
Fe[a]	1.217	1.126	1.079	1.156	1.221	1.098
Mn	0.000	0.000	0.000	0.005	0.007	0.004
Ca	0.000	0.000	0.000	0.000	0.006	0.000
Na	0.009	0.013	0.012	0.013	0.021	0.007
K	0.910	0.884	0.890	0.968	0.946	0.826
Ba	0.002	0.000	0.001	0.005	0.007	0.006
F	0.107	0.115	0.120	NA[b]	NA	0.123
Cl	0.044	0.049	0.012	NA	NA	0.016
Oxide sum	95.55	95.77	94.91	94.79	94.97	94.64

[a] All measured Fe calculated as ferrous iron.
[b] Not analyzed.

away from the dike are uniformly about 0.4 wt%. Grains in the contact zone with the dike have somewhat more variable F contents in the range 0.4 to 1.0 wt%.

Spinel is iron rich, with mole fraction of hercynite component ($Fe^{2+}/Fe^{2+}+Mg+Zn$) between 0.70 and 0.84. Zinc content, expressed as mole fraction of gahnite component (Zn/Fe^{2+}

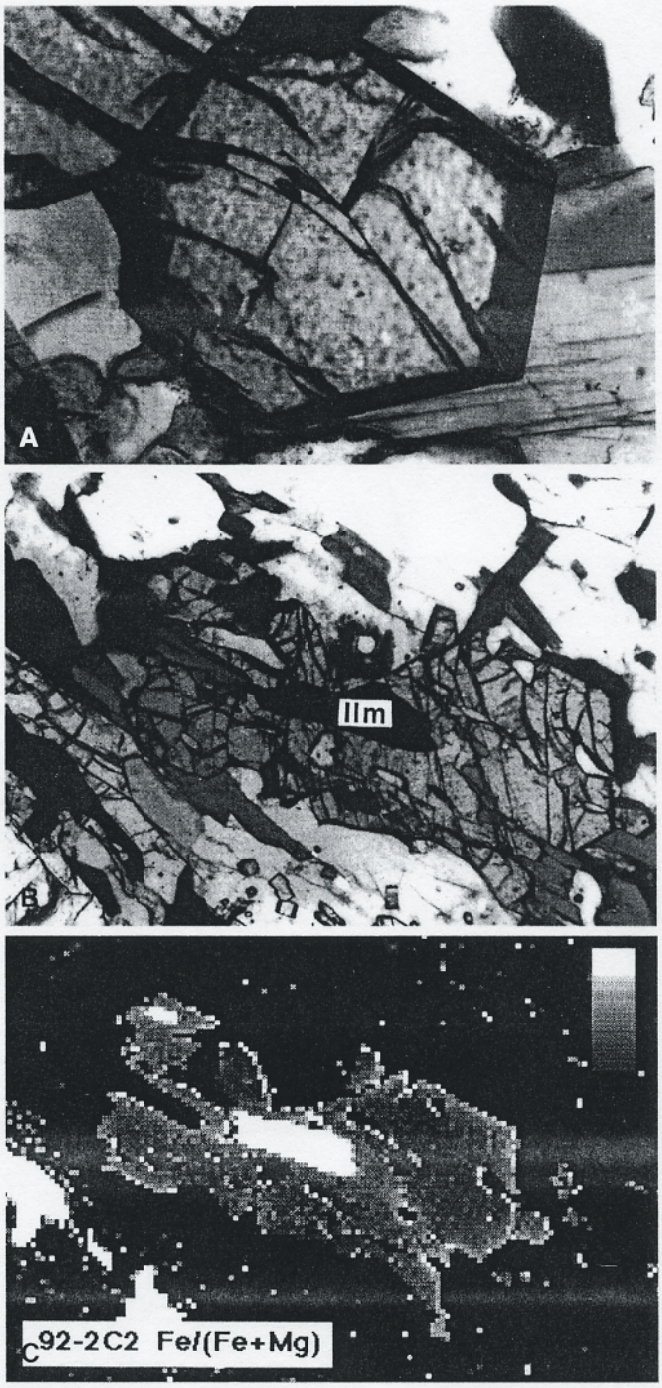

Fig. 3 **A** Photomicrograph of a small garnet neoblast with euhedral morphology and well defined dodecahedron faces in sample 92-2C2. Width of photo 0.5 mm. **B** Photomicrograph of another garnet in sample 92-2C2 with faceted margin on right side. The grain contains a large inclusion of ilmenite and a number of smaller inclusions of quartz and biotite. Width of photo 1.5 mm. **C** X-ray map of garnet (in **B**) showing the variation in Fe/(Fe+Mg). *Bright regions* along grain margins show increased Fe relative to the core, which is most pronounced on the right side where the garnet is adjacent to biotite. There is also a region of higher Fe around a small biotite inclusion in the garnet. The *bright zone* in the central portion of the garnet is the included grain of ilmenite

+Mg+Zn), ranges between 0.03 and 0.36. Consistently low Zn-contents were measured from hercynite grains in assemblages with low Mn concentrations in garnet (X_{Sps} = 0.01–0.03), whereas the highest gahnite values were measured from samples with relatively spessartine-rich garnets (X_{Sps} = 0.15). No zoning in Zn, Fe, or Mg was recognized in the spinels. Visible 1–3 μm exsolution lamellae of magnetite were present in some grains, particularly in regions with late chlorite alteration. The presence of a component of Fe^{3+} is stoichiometrically indicated in virtually all hercynite analyses.

Corundum and sillimanite analyses also show detectable abundances of ferric iron. Corundum inclusions in garnet had trace amounts of Fe^{3+}, and up to 0.5 wt% was measured in inclusions in hercynite and ilmenite. Sillimanite associated with the melt-texture veins also had between trace amounts and 0.5 wt% Fe^{3+}. There is no measurable ZnO in either corundum or sillimanite.

Crystallization history during anatexis

We have used the textural information described above to infer a sequence of mineral crystallization associated with the partial melting of the gneiss. The earliest formed mineral paragenesis preserved in these rocks appears to have included K-feldspar, sillimanite, biotite, garnet, plagioclase, quartz, and ilmenite. Corundum inclusions are present in both garnet and hercynite, although it is never seen in the matrix. Since there is abundant quartz in the gneiss, it is not likely that corundum was a stable matrix phase. Corundum inclusions in garnet and ilmenite may have formed during breakdown of biotite or as these phases crystallized directly from a highly aluminous melt. Corundum is often seen partly altered to or surrounded by hercynite. These textures suggests that the reaction

corundum + garnet = hercynite + sillimanite (1)

formed some of the hercynite now present as inclusions in garnet. Hercynite in the matrix was likely produced by the reaction

garnet + sillimanite = hercynite + quartz (2)

which lies to the high-temperature side of the corundum-out reaction (Bohlen et al. 1986). The thin rims of either sillimanite or garnet presently separating hercynite and quartz in most samples were likely formed by retrograde reaction.

Mineral textures suggest that the high temperature event that stabilized the hercynite + quartz assemblage also initiated melting. The feldspar-sillimanite-quartz veins that surround partly reacted biotite also mantle ilmenite and hercynite, which may indicate that melting occurred at temperatures above the first appearance of hercynite. The crystallization of faceted garnets and K-feldspar surrounding grains of quartz demonstrate that biotite-dehydration melting operated under vapor-absent conditions for at least a portion of the melting interval.

P-T conditions of partial melting

Despite evidence for a polymetamorphic history, it is possible to estimate conditions at the onset of anatexis in the metapelitic gneiss by considering the mineral suite that texturally defines the melting episode. The melt composition was strongly peraluminous, as indicated by the coexistence of abundant sillimanite and plagioclase in the melt-texture veins. Experimental studies have demonstrated that peraluminous melt compositions are formed by solidus reactions that involve the breakdown of muscovite and biotite (e.g., Clemens and Wall 1981; Vielzeuf and Holloway 1988; LeBreton and Thompson 1988; Patino Douce and Johnson 1991). All the pelitic gneiss samples in the vicinity of Port Leyden contain abundant biotite, but none have muscovite. In rocks where melt-texture veining is observed, it cuts across a matrix of coarse-grained K-feldspar, which indicates that sillimanite and K-feldspar were already stable relative to quartz and muscovite at the time of melting. Consequently, we do not feel that an initial melting reaction involving muscovite was likely. A more probable melting reaction involved the dehydration of biotite, either under vapor-present or vapor-absent conditions, according to

biotite + sillimanite + vapor = garnet + melt (3)

or

biotite + sillimanite + quartz = garnet ± K-feldspar + melt (4).

Experimental studies of these equilibria give temperature estimates of between 700 and 770° C for initial melt generation by vapor-absent biotite dehydration for pressures up to about 7 kbar (Clemens and Wall 1981, LeBreton and Thompson 1988). We therefore propose that the temperature range 700–770° C is a reasonable estimate of the temperatures of metamorphism for these rocks at the time of initial melting. Temperatures in this range account for the melt-related textures in the reactant and product phases, but do not imply advanced melting reactions involving additional ferromagnesian phases, such as orthopyroxene, which have not been recognized in these rocks.

Coexistence of quartz and Fe-spinel in the metapelites provides a useful constraint on the pressure conditions of metamorphism through consideration of the reaction

almandine + 2 sillimanite = 3 hercynite + 5 quartz (5).

This reaction has been experimentally examined by Bohlen et al. (1986) in the FAS system and by Nichols et al. (1992) for Fe-Mg-Zn solid solution. Results of these studies show that the assemblage defines a positively sloping reaction surface in *P-T* space that is strongly dependent on pressure and is therefore suitable as a geobarometer if temperature is known to within ±50° C. Hercynite and almandine contents were mea-

sured from nearby but non-touching grains. The solution model for the activity of hercynite was taken from Nichols et al. (1992). In order to calculate the hercynite component, Fe^{2+} was estimated by distributing the total measured iron between octahedral and tetrahedral sites assuming charge balance. The magnetite component calculated in this way amounts to between 4 and 6 mol%. The presence of a small amount of Fe^{3+} in hercynite has the effect of increasing its stability field relative to garnet + aluminum silicate. However, this displacement to the equilibrium is partially canceled by the Fe^{3+} in sillimanite. Core compositions from garnet were selected for thermobarometry in order to minimize the effects of retrograde modification to Fe and Mg concentrations. Nonideal corrections for mixing in garnet were determined using the model of Berman (1990). Calculations made using the experimental results and thermodynamic data from these studies yielded the range of *P-T* estimates shown in Fig. 4. For an assumed range of temperatures between 700 and 770° C, calculated pressures are between 3.7 and 6.4 kbar.

Because Fe and Mg gradients in garnet point to the reequilibration of Fe/Mg partitioning throughout the sample, it is appropriate to consider the significance of our pressure estimates in the light of possible compositional modifications. For example, if chemical diffusion during slow cooling led to an increase of almandine concentration in garnet cores as well as garnet rims, estimates based on reaction (5) using core compositions would give overestimated pressures at any given temperature. Specifically, if the garnet composition in equilibrium with hercynite at the time of melting had an X_{Alm} 0.05 lower than presently measured in core regions, the pressure range we estimated would be decreased by about 0.3 kbar. However, garnet porphyroblasts with 0.75 mm and greater radius have uniform of core compositions, suggesting that diffusion-induced changes are restricted to rim regions. Hercynite grains show no compositional zoning, but their small size suggests that reequilibration effects could be homogeneous. Again, we can speculate on the possible effect of such changes. If hercynite became enriched in Fe relative to its composition at the time of melt production, pressures would be underestimated. Specifically, an increase of 0.05 in X_{Hc} will introduce 0.8 kbar error into our calculations.

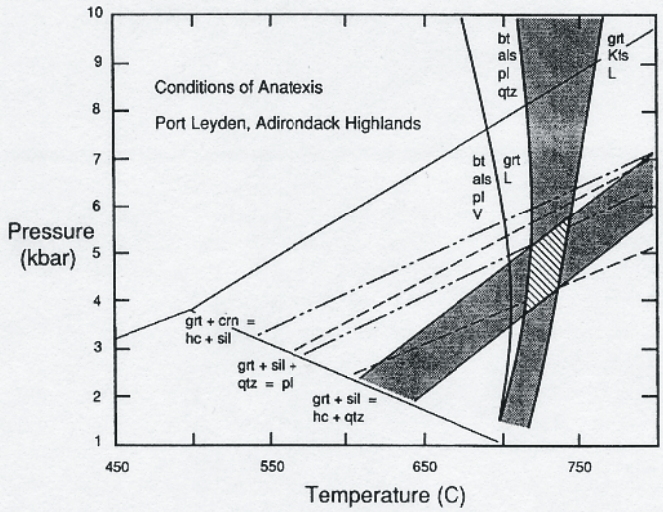

Fig. 4 *P-T* diagram with phase equilibria constraints for conditions of anatexis in the metapelitic gneiss at Port Leyden. A range of temperatures between about 700 and 770° C is shown for vapor-absent biotite dehydration melting (Clemens and Wall 1981; LeBreton and Thompson 1988). *Dot-dash patterned lines* delimit the reaction garnet + corundum = hercynite + sillimanite. *Dashed lines* show the range for the equilibrium garnet + sillimanite + quartz = plagioclase. The pressure of metamorphism and anatexis is defined by the coexistence of hercynite spinel and quartz and the temperature range of partial melting. Mineral symbols after Kretz (1983)

Metamorphic pressures can also be estimated through compositional relations governed by the equilibrium

3 anorthite = grossular + sillimanite + quartz (6).

Anorthite content was obtained from homogeneous, granoblastic grains of plagioclase in the melt veins, and grossular activity was determined from garnet compositions of the small euhedral grains assumed to have grown in equilibrium with the melt. Although all garnets have retrograde compositional zoning in Fe and Mg, grossular concentration is essentially constant from center to rim in each crystal and uniform from grain to grain. Furthermore, the absence of embayments or irregularities on the faceted surfaces argues against any significant involvement of garnet in subsolidus net transfer retrograde reactions. Consequently, we are reasonably confident that the grossular content in the interior of the euhedral garnet grains has been unmodified since crystallization. Pressure estimates between 4.5 and 7.7 kbar for assumed temperatures of 700 to 770° C were obtained by applying the Koziol and Newton (1988) calibration of reaction (6). Alternative calibrations of the GASP geobarometer lead to some variation in calculated absolute pressures. For example, estimates determined with the calibration of Ganguly and Saxena (1984) gave a slightly expanded range of pressures and the calibration of Newton and Haselton (1981) yielded pressures 0.5 to 1.5 kbar less. The generally good agreement between hercynite-quartz barometry and GASP geobarometry is consistent with the assumption that equilibrium was simultaneously achieved between components in garnet, plagioclase, and spinel.

The significance of the GASP barometry estimates must also be evaluated in light of the later metamorphic episode that these rocks experienced, which could have altered the compositions of both plagioclase and garnet. Because both these phases have very slow diffusivities of calcium components (Grove et al. 1984; Chakraborty and Ganguly 1992), it is not likely that volume diffusion produced significant modification to the Ca distribution in mineral grains that crystallized at the time of anatexis. A more substantial concern arises over whether later operation of net transfer reaction (6) caused compositional changes (Spear and Florence 1992). It this is the case,

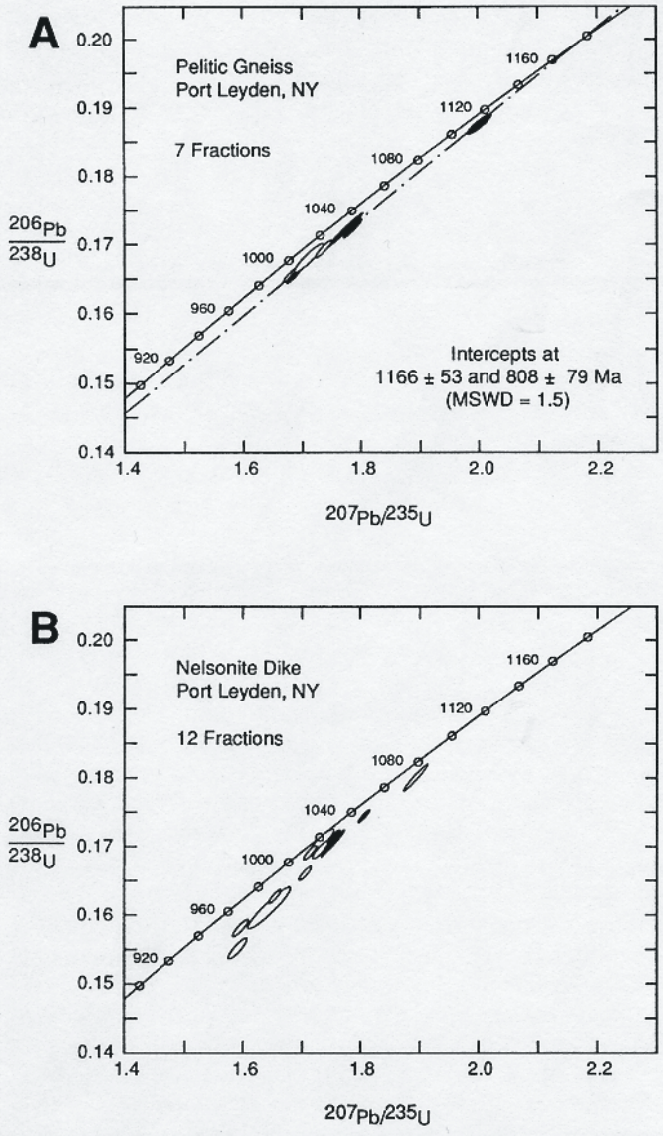

Fig. 5A, B U-Pb concordia diagrams for zircon fractions from two Port Leyden rocks. *Ellipses* represent 2 σ analytical uncertainty. *Open ellipses* single grain measurements, *solid ellipses* multiple grain fractions. **A** Metapelite gneiss. The upper intercept age of 1166±53 Ma dates the timing of anatexis. **B** Nelsonite intrusion. The non-linear array contains an inflection at about 1020 Ma, which corresponds to a lead-loss event. Notice the near concordance of two multiple grain and three single grain analyses at this age

mass balance requirements (for an assumed closed system) lead to the prediction that the greatest changes would occur in the grossular zoning in garnet if plagioclase throughout the samples was highly reactive during later metamorphism. At the same time, this would minimize the compositional changes in plagioclase. Conversely, if only a small percentage of the plagioclase in these rocks reacted during later metamorphism, newly formed plagioclase could have a significantly different composition, but changes to garnet zoning would be slight. At Port Leyden, we have observed nearly flat zoning profiles in grossular and nearly constant An values in plagioclase (outside of the contact zone), which indicates that there has not been extensive progress of the GASP reaction since the partial melting event. Patchy zoning and albite rims on plagioclase in sample BD-03b may be evidence for a limited amount of reaction accompanying late metamorphism. However, for our present purposes we are concerned with the earlier compositions of plagioclase and garnet, which appear to have essentially unmodified contents of calcium components.

The results of thermobarometry calculations are summarized in Fig. 5, along with stability fields for the observed coexisting assemblages. Based on the agreement between mineral equilibria, we conclude that melting took place between 4.0 and 6.4 kbar.

P–T conditions of later metamorphism

There is only limited evidence for late metamorphic net transfer reactions involving silicate and oxide minerals. The presence of idioblastic biotite grains indicates some progress of the hydration reaction

garnet + K-feldspar + H_2O = biotite and sillimanite (7).

However, garnet neoblasts do not show resorption textures, and there is no evidence for breakdown of K-feldspar, which suggests that the abundance of biotite formed by this reaction may not have been great. The few rutile overgrowths observed on hercynite may have formed from TiO_2 liberated during biotite recrystallization, or conceivably according to the vapor-absent reaction

ilmenite + aluminum silicate + quartz = garnet + rutile (8).

This reaction is the basis of the GRAIL geobarometer (Bohlen et al. 1983), suggesting that this assemblage can be used to obtain pressure information related to later metamorphism. However, Fe-Mg exchange during cooling has modified components in garnet rims and biotite and, presumably, ilmenite. The absence of preserved Fe/Mg equilibria related to the high grade conditions of later metamorphism argues against applying GRAIL geobarometry in these rocks.

Similarly, the thermal maximum of the later metamorphic event is not constrained by equilibrium mineral partitioning. Temperatures calculated from garnet-biotite thermometry range between 550 and 600° C using garnet core compositions and 500–550° C using garnet rims. If we are correct in assuming that in the larger grains garnet core compositions were not significantly modified from the time of anatexis, then the temperatures obtained through exchange thermometry imply a substantial shift in Fe/(Fe+Mg) in biotite.

In order to shed some light on the thermal conditions of later metamorphism, we constructed numerical mod-

els of cooling rates based on Fe/Mg diffusional zoning in euhedral garnet neoblasts (Lasaga 1983). Our logic was to see if we could recognize a temperature-time (T-t) history for these rocks that compared with the T-t evolution of the Adirondack highlands formulated by Mezger et al. (1991) on the basis of U-Pb geochronology. Starting temperatures of between 625 and 775° C were assumed in different cooling simulations. Starting conditions included assumed core compositions equal to that found in >2 mm diameter garnet (X_{Alm} = 0.77) and a volume ratio of garnet to biotite = 0.10. Intergranular diffusion, and diffusion in biotite, were assumed fast relative to intragranular diffusion in garnet. Temperature-composition dependent interdiffusion coefficients were calculated from the tracer diffusion data of Chakraborty and Ganguly (1992). No cooling rates yielded good matches to the garnet Fe/(Fe+Mg) profile at starting temperatures of 700° C or less. A best match was obtained assuming initial conditions of 750° C and a constant cooling rate of 1.5° C/Ma. Despite the lack of definable precision to this approach, the model T-t evolution is in excellent agreement with the post-Ottawan cooling history determined from geochronology in the central Highlands, and suggests that comparable thermal conditions of metamorphism were achieved in the western Adirondacks.

Nelsonite intrusion

The metapelitic unit is host to a distinctive dike composed of 32–50% magnetite, 8–15% ilmenite, 30–45% apatite, and 5–11% pyrite (Darling and Florence 1995). This uncommon rock type, designated nelsonite, is known to originate as an immiscible liquid from anorthosite-ferrodiorite melts (Philpotts 1967; Epler 1987). Field relations and mineral textures confirm the intrusive character of the Port Leyden nelsonite. The intrusion forms a sharp-walled dike 4 m wide that can be traced for approximately 30 m as a discordant body intruding nearly vertically into the surrounding, moderately dipping metapelitic gneiss (LaForce et al. 1994). At the contact between the host gneiss and the dike there is a 0.5 to 1.0 cm wide reaction zone of very coarse, red-brown biotite. Similar coronas surround small xenoliths entrained in the dike rock. Xenoliths contain symplectites of plagioclase and quartz, garnet, rutile, monazite, and chlorite alteration, especially around plagioclase. There is a sharp increase in the model abundance of plagioclase in the pelitic gneiss within about 2 cm of the contact. Plagioclase abundance increases over a distance of 10 cm from less than 5% to more than 50 to 90% of the wall rock and plagioclase-quartz symplectites formed immediately adjacent to sieve-textured biotite in the contact zone.

The nelsonite dike is fine-grained (0.1 to 0.5 mm) and has an overall mosaic texture. Magnetite and apatite form equant grains, whereas ilmenite occurs as coarser, interstitial, optically continuous grains. These textures are considered to be primary and igneous. The rock also shows a weak foliation defined by flattened stringers of pyrite crystals, which we interpret to be the result of partial metamorphic recrystallization. Electron microprobe analysis disclosed that some apatite grains contain sharp compositional discontinuities, especially where in contact with pyrite. These grains have thin (ca. 20 μm) rims with distinctly lower REE abundances relative to cores. In the light of the very slow diffusivities of REE in apatite (Watson et al. 1985) it is likely that the apatite rims recrystallized during post-intrusion metamorphism.

Ages of metamorphism

In order to clarify the timing of dike intrusion, anatexis, and younger metamorphism, U-Pb age determinations were made at the isotope geochemistry laboratory at Syracuse University using zircon and monazite from the nelsonite dike and the pelitic gneiss (see Appendix for analytical procedures). Mineral populations from each rock selected for geochronology were separated into distinct fractions on the basis of morphological characteristics.

Zircons separated from the nelsonite included prismatic crystals less than 0.3 mm long, subhedral, cylindrical grains up to 0.75 mm long, and irregular shaped and rounded grains. Thin, discontinuous overgrowth rims were recognized on zircons in thin sections of nelsonite when viewed with backscattered electron imaging. Isotopic measurements were taken on air abraded single grains and multiple grain fractions separated by size and magnetic susceptibility. U-Pb ratios from the zircon population of the nelsonite produce a non-linear array with a nearly concordant inflection at about 1020 Ma (Fig. 5, Table 2). A $^{207}Pb/^{206}Pb$ age from an air abraded single prism provides a minimum age constraint of 1104±3 Ma. While it is possible to force a regression through points above the inflection, the large uncertainty associated with the upper intercept makes the determined age highly questionable. However, the significance of the nearly concordant inflection is supported by the very close coincidence of the results from five fractions. The ca. 1020 Ma age appears to date an episode of radiogenic lead loss from earlier formed zircons, as well as the timing of recrystallization and resorption that produced overgrowth textures on zircon prisms and the irregular morphology seen in many grains. We believe that formation of these textures coincided with the development of the metamorphic fabric in the dike and the partial recrystallization textures recognized in apatite. It appears likely that the 1020 Ma zircon date from the nelsonite corresponds with the age of Ottawan metamorphism in the Highlands established by Mezger et al. (1991).

The significance of the older zircon ages is less certain. It is possible that they reflect some inheritance in older cores that pre-dates the timing of dike intrusion.

Table 2

Summary of U-Pb analytical results and mineral ages

Fraction	Weight	Concentrations			Atomic Ratios								Ages (Ma)			
		U	Pb[a]	Total Common	$^{206}Pb^{b}$	$^{208}Pb^{c}$	$^{206}Pb^{c}$	Error	$^{207}Pb^{c}$	Error	$^{207}Pb^{c}$	Error	^{206}Pb	^{207}Pb	^{207}Pb	
	(mg)	(ppm)	(ppm)	Pb (pg)	^{204}Pb	^{206}Pb	^{238}U	(%)	^{235}U	(%)	^{206}Pb	(%)	^{238}U	^{235}U	^{206}Pb	rho
Nelsonite zircons																
1 AA prism	0.008	491	94	37	653	0.134	0.18026	0.831	1.89980	0.869	0.07636	0.252	1068.4	1080.4	1104.6	0.957
7 prisms	0.113	1147	204	600	1970	0.094	0.17507	0.513	1.80464	0.542	0.07476	0.175	1040.0	1047.1	1062.1	0.947
1 metamict	0.050	307	51	39	1765	0.073	0.16644	0.570	1.70411	0.600	0.07426	0.188	992.5	1010.1	1048.5	0.950
1 AA prism	0.008	200	31	6.1	916.9	0.090	0.15541	0.833	1.59113	0.884	0.07426	0.295	931.2	966.7	1048.4	0.953
4 AA prisms	0.020	237	40	1.9	2343	0.059	0.17138	0.853	1.74975	0.871	0.07405	0.175	1019.7	1027.1	1042.8	0.980
1 lg prism	0.015	402	65	19	453.7	0.073	0.16120	1.85	1.64573	1.950	0.07404	0.626	963.5	987.9	1042.6	0.947
Mult round	0.031	4986	863	260	4464	0.090	0.17200	0.516	1.75154	0.541	0.07386	0.161	1023.1	1027.7	1037.5	0.954
1 AA round	0.019	189	33	28	886.1	0.098	0.17043	0.622	1.73320	0.681	0.07376	0.273	1014.5	1020.9	1034.8	0.916
1 AA prism	0.031	644	118	160	1045	0.203	0.16291	0.515	1.65281	0.553	0.07358	0.200	972.9	990.6	1030.0	0.932
1 AA prism	0.008	388	67	7.9	815.9	0.094	0.17057	1.07	1.73182	1.160	0.07356	0.423	1016.3	1020.4	1029.4	0.931
1 AA prism	0.008	336	56	5.4	1746	0.065	0.16941	0.606	1.71345	0.645	0.07336	0.220	1008.9	1013.6	1023.8	0.940
1 anhedral	0.032	858	136	120	1248	0.068	0.15875	0.705	1.59788	0.748	0.07300	0.245	949.8	969.4	1014.0	0.945
Pelite zircons																
1 lg round	0.012	380	76	50	624.8	0.127	0.18777	0.773	2.00150	0.833	0.07731	0.302	1109.3	1116.0	1129.2	0.932
1 AA round	0.016	166	30	19	744.8	0.103	0.17200	0.800	1.77819	0.833	0.07498	0.231	1023.1	1037.5	1068.0	0.961
6 prisms	0.010	325	53	3.2	570.8	0.037	0.17156	1.63	1.76346	1.66	0.07455	0.310	1020.7	1032.1	1056.4	0.982
20 med round	0.025	295	49	57	847.2	0.046	0.16874	0.636	1.72492	0.742	0.07414	0.373	1005.1	1017.9	1045.3	0.865
1 lg prism	0.009	413	65	10	1779	0.034	0.16480	0.570	1.67520	0.660	0.07372	0.330	983.4	992.2	1033.9	0.866
1 lg round	0.010	247	44	37	504.0	0.099	0.16816	1.23	1.70842	1.30	0.07368	0.424	1002.0	1011.7	1032.8	0.945
50 sm round	0.020	360	56	11	1610	0.020	0.16507	0.665	1.67310	0.712	0.07351	0.249	984.9	998.4	1028.0	0.937
Nelsonite monazites																
Single	0.097	223	518	550	3344	0.509	0.17001	1.75	1.66428	1.80	0.07100	0.420	1012.2	995.0	957.4	0.973
Single	0.033	384	25	62	538.3	0.342	0.05151	0.577	0.49979	0.638	0.07037	0.266	323.8	411.6	939.2	0.909
Single	0.038	321	38	20	890.7	2.230	0.04131	0.699	0.39948	0.738	0.07013	0.233	261.0	341.3	932.2	0.949
Pelite monazites																
Single	0.053	1714	218	13	5767	2.51	0.04094	0.488	0.41924	0.514	0.07427	0.159	258.7	355.5	1048.9	0.951
Single	0.043	1168	237	59	1580	4.67	0.04039	0.609	0.41238	0.636	0.07406	0.184	255.2	350.6	1043.0	0.957
60 small	0.095	1767	509	120	5791	2.62	0.09003	0.499	0.91849	0.524	0.07399	0.159	555.7	661.6	1041.2	0.953
Single	0.031	1087	490	27	2858	4.71	0.08984	0.757	0.91626	0.777	0.07397	0.172	554.6	660.4	1040.5	0.975
Single	0.017	1994	290	8.3	4795	2.11	0.05273	0.583	0.53774	0.608	0.07396	0.173	331.3	436.9	1040.3	0.959
Single	0.041	1947	256	110	1611	2.42	0.04314	0.540	0.43808	0.573	0.07365	0.190	272.3	368.9	1031.9	0.994

[a] radiogenic Pb
[b] measured ratio is corrected for fractionation and spike only
[c] measured ratio is corrected for fractionation, spike, blank, and initial common Pb

However, relict core regions were not observed in any grains viewed with backscattered imaging electron. Furthermore, if relict cores were present in the analyzed grains, one might expect air abrasion to produce systematically older ages, reflecting greater concentrations of core material. As can be seen from the data (Table 2), such systematic behavior was not found. Alternatively, the almost universal association of Fe-Ti oxide-apatite nelsonite with anorthosite suite rocks implies that the dike was intruded during anorthosite magmatism. Thus, we feel it is more likely that the zircon population giving older ages represents grains that crystallized at the time of anorthosite magmatism, then experienced subsequent modification to their U-Pb systematics. In support of this hypothesis we point to (a) the lack of any minimum age determinations older than the time of anorthosite suite magmatism, and (b) the strong similarity in the results from the nelsonite with the characteristics reported for 'disturbed' zircon populations by Chiarenzelli and McLelland (1993) from other AMCG rocks in the Highlands. These workers postulated that radiogenic lead loss during granulite facies metamorphism creates a short, discordant array of zircon dates between the age of crystallization and the timing of granulite facies metamorphism. Subsequent lead loss shifts the discordant position of individual analyses, forming a complex, "dog-leg" pattern.

Zircons from the pelitic gneiss included prisms with subhedral grain shapes and overgrowth textures and small (0.05–0.20 mm), multifaceted grains with low aspect ratios. Discordant U-Pb data were obtained from analyses of different size fractions and single grains of prisms and multifaceted zircons (Table 2). The $^{207}Pb/^{206}Pb$ ratio from an air abraded single grain with a stubby, multifaceted morphology gives a minimum age of 1129±6 Ma. A linear regression through all fractions gives an upper intercept age of 1166±53 Ma. An upper intercept at 1165 Ma is obtained by regression through the single grain analyses only. We interpret these results as minimum and maximum constraints, respectively, on the age of older metamorphism in the gneiss. The interval 1166–1129 Ma is essentially contemporaneous with the widespread AMGC magmatism in the Adirondacks and suggests that heating accompanying this magmatic event was responsible for metamorphism in the gneiss.

This interpretation is predicated on the assumption that zircon grains in the gneiss do not contain U-Pb inheritance from detrital components. A number of observations support this conclusion. The high aluminum content of the gneiss suggests that the protolith was a clay shale. Presumably, then, any zircon deposited with the clay fraction would have been micron-scale, far smaller than the grains we separated. When examined with a binocular microscope, the grains appear to be clear, colorless, and inclusion-free. Their small, stubby to equidimensional, multifaceted morphology is similar to zircon grains from intrusions of the AMCG suite that Chiarenzelli and McLelland (1993) interpreted as metamorphic in origin. All of the grains we analyzed contained relatively low abundances of uranium, which also compares with the metamorphic grains studied by Chiarenzelli and McLelland (1993). Finally, petrographic study of the gneiss indicates that most zircon crystals are present in and adjacent to melt textured veins. We suggest, therefore, that either these grains crystallized contemporaneously with partial melting or experienced nearly complete radiogenic lead loss at this time, so that their age coincides with the timing of anatexis.

Ottawan metamorphism does not appear to have affected zircons from the gneiss in the same way as in the nelsonite. For example, zircons from the gneiss do not show the resorption and recrystallization textures found in the nelsonite population. Also, the linear array of ages from the gneiss zircons contains no evidence for new zircon growth or substantial radiogenic lead loss associated with a 1020 Ma metamorphic episode. Partial lead loss during younger metamorphism may be reflected in the lower intercept age of 808±79 Ma.

Monazite U-Pb ages constrain the timing of younger metamorphism in the gneiss. Six fractions of monazite were obtained from gneiss sampled about 0.5 km from the dike (location BD-03b). These yield a linear regression with an upper intercept of 1041±9 Ma (Fig. 6). This age is slightly older than the zircon U-Pb age for Ottawan metamorphism obtained from the nelsonite. The closure temperature for monazite has been estimated to be between 650 and 700° C (Parrish 1988) or up to 750° C (Copeland et al. 1988). Chiarenzelli and McLelland (1993) suggest that closure temperatures for zircon in slowly cooled terranes may be as low as 750° C. Assuming that both the nelsonite zircon and pelite monazite ages reflect closure temperatures, these results indicate that temperatures following Ottawan metamorphism in the western Adirondacks reached between 650 and 750° C at approximately the same time as in the central Highlands (1033±1 Ma; Mezger et al. 1991).

A younger monazite age was obtained from three grains separated from the dike. All monazites from the nelsonite have low uranium abundances and two are strongly discordant in a normal sense, while one grain is reversely discordant (Fig. 6). A linear fit to the data points gives an upper intercept age of 957±8 Ma. We consider this to be a minimum age, and suggest that if reverse discordance indicates the presence of excess thorium, the $^{207}Pb/^{235}U$ age of 995 Ma may also be a minimum age.

The close proximity of the nelsonite and gneiss sample sites, and the absence of any known structural discontinuity between them, argues against there having been markedly different thermal histories for the two rocks. Monazite grain sizes in each rock were similar (<0.5 mm), so there is no reason for inferring different closure temperatures for the two monazite populations based on surface area/volume considerations. Monazite grains in the dike tend to be anhedral and irregularly shaped and they occur interstitially to apatite and Fe-Ti oxides. These textures, as well as the compositional vari-

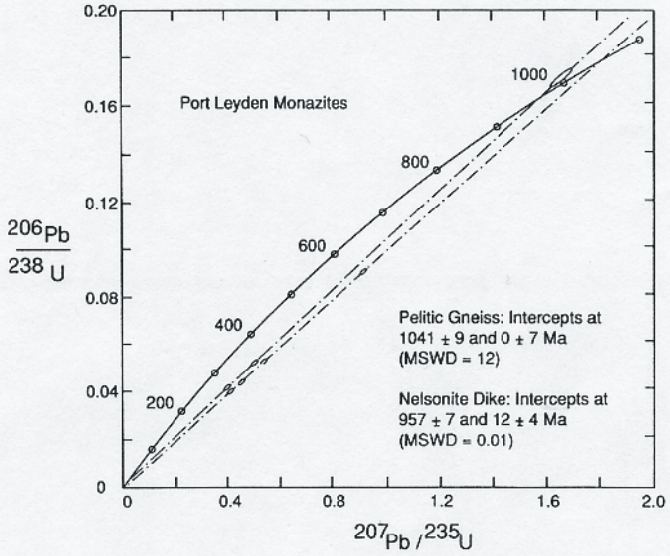

Fig. 6 U-Pb concordia diagram for monazite fractions from pelitic gneiss and nelsonite. Regression for the upper intercept age from the nelsonite dike includes one reversely discordant grain, and the age may represent a minimum age. *Ellipse* for reversely discordant grain from the nelsonite dike represents 2 σ analytical uncertainty. *Ellipses* for all other grains exceed 2 σ error, but are enlarged for clarity

ations between LREE-rich cores and thin LREE-depleted rims in apatite, indicate that post-emplacement reaction of apatite formed monazite in the nelsonite. It is therefore possible that the discrepancy between the gneiss and dike monazite ages reflects late crystallization of monazite in the nelsonite dike.

Discussion

Reported occurrences of nelsonite establish that this rock type is intimately associated with or proximal to anorthositic and ferrodioritic intrusives (Philpotts 1967; Kolker 1982). Experimental evidence supports a model of differentiation of anorthosite magma that yields a ferrodiorite melt enriched in titanium and phosphorus, from which the immiscible Fe-Ti oxide-apatite liquid eventually separates (Philpotts 1967; Epler 1987). The REE chemistry and the mineralogy of the nelsonite at Port Leyden are indistinguishable from those in nelsonites that are part of anorthosite suites elsewhere (Darling and Florence 1995). What appears to be the exceptional characteristic of the Port Leyden dike is the absence of a closely situated anorthosite or ferrodiorite pluton.

In fact, we believe that the presence of the nelsonite dike within the Port Leyden metapelites is strong evidence that an anorthosite pluton was intruded into the metasedimentary sequence close to the level of the rocks now exposed. Furthermore, the agreement of the age determinations from metamorphic zircon in the pelitic gneiss, and the timing of anorthosite magmatism elsewhere in the Adirondacks, suggest to us that igneous activity at about 1150 Ma was responsible for heating and anatexis of the metasediments. Simple conductive heat flow calculations show that the dike itself was incapable of melting rocks more than tens of cm to a few m from its contacts, and it is therefore not reasonable that the nelsonite intrusion produced the melt textures observed over tens of km^2 of outcrop around Port Leyden. However, the distribution of anatectic veining may be adequately explained by postulating the nearby intrusion of a significant volume of anorthosite and related magmas. The absence of even small outcrops of anorthosite or ferrodiorite within about 50 km of the Port Leyden nelsonite suggests to us that the parent magma was emplaced above the stratigraphic level of currently exposed rocks and then subsequently removed by erosion or tectonism. (Considering that the average density of the dike is approximately 4300 kg/m^3, we envision that the nelsonite was intruded downward from its parent magma.) If this hypothesis is correct, the pressure estimates developed here give a range of about 13 to 19 km for the maximum depth of intrusion of anorthosite suite rocks in the western Adirondack Highlands. These geobarometric results broadly corroborate isotopic evidence presented by Valley and O'Neil (1982) for upper crustal depths of emplacement for anorthosite plutons in the Adirondack Highlands.

The discovery of moderate pressure metamorphism in the Port Leyden region also helps clarify the relative crustal depths of the Highland and Lowland terranes during the Grenville Orogeny. The Adirondack Lowland portion of the Frontenac Terrane lies to the west of the Adirondack Highlands, separated from it by the Carthage-Colton Mylonite Zone. Upper amphibolite to granulite facies metamorphism characterizes the Lowlands, and pressures of between 5.4 kbar to the south and 8.0 kbar to the north have been estimated from several silicate and oxide thermobarometers (Bohlen et al. 1985; Powers and Bohlen 1985; Edwards and Essene 1988). Geochemical and geochronological studies of granitic and syenitic plutons in the Lowlands (Chiarenzelli and McLelland 1991; Carl and Sinha 1992; McLelland et al. 1993) have demonstrated that they are temporally and compositionally equivalent to the AMCG suite in the Highlands. Thus, the Highland and Lowland regions appear to have been part of a common terrane during AMCG magmatism. Subsequent thermotectonic events affected these regions differently, as indicated by the sharp geochronologic discontinuity that has been recognized across the Carthage-Colton Mylonite Zone (Mezger et al. 1991, 1992). Mezger et al. (1991) determined that closure ages for garnet, monazite, and titanite extended from 1170 to 1100 Ma across the Lowlands, but, in contrast to the Highlands, found no geochronologic record of the younger Ottawan Orogeny in this region. It is therefore probable that the metamorphic *P-T* estimates for the Lowlands reflect conditions that prevailed there at about the same time as the emplacement of the AMCG rocks in the Highlands.

Metamorphic pressures at Port Leyden and in the southern and southeastern Lowlands from the time of AMCG magmatism are, within uncertainty, equivalent, indicating that these regions were positioned at similar crustal depth of about 1150 Ma. However, there has been no identified trend of northward increasing pressure in the Highlands as appears to exist in the Lowlands. The wollastonite skarns in the northeast, central, and western Highlands are all interpreted to have formed from contact metamorphism at this time (Valley et al. 1990), presumably at moderate to low pressure conditions. It is possible, then, that portions of the Highlands were situated at shallower crustal depths than at least the northern Lowlands when the AMCG plutons were intruded. By about 1040 Ma the relative depths of these terranes were either reversed, or the terranes were separated in some way that prevented the Lowlands from experiencing the high temperature conditions that prevailed in the Highlands. Much of the Highlands appears to have experienced granulite facies metamorphism at 7 kbar pressure. The Lowlands, in contrast, occupied a higher crustal position where Ottawan metamorphism did not reset U-Pb systematics in titanite (Mezger et al. 1991, 1992), that is, where temperatures remained less than about 500–550° C.

Conclusion

Mineral compositions and melt textures in pelitic rocks that are host to a nelsonite dike demonstrate that pressure conditions of about 4 to 6 kbar existed in the western Adirondack Highlands during intrusion of AMCG suite rocks. This pressure estimate is considerably less than the 7 to 8 kbar pressures reported by Bohlen et al. (1985) elsewhere in the Highlands for granulite facies metamorphism. However, those higher pressures are likely related to ca. 1050–1000 Ma Ottawan age metamorphism, whereas the pressure estimates described here derive from localized preservation of mineral assemblages formed during ca. 1150 Ma thermal metamorphism. The general lack of clear petrologic evidence throughout much of the Highlands of the thermobaric conditions at the time of AMCG magmatism suggests that exceptional conditions prevailed around Port Leyden in order to preserve the textures and mineral chemistry of these samples. Buddington (1939) first recognized that igneous rocks in the western Adirondacks were distinguished by their relatively undeformed textures, and our observation that extensive recrystallization did not affect minerals and textures in the pelitic gneiss since the time of AMCG magmatism is consistent with this observation.

Although extensive Ottawan age deformation is not indicated in these rocks, metamorphic temperatures of at least 700° C at 1040 Ma are indicated by the closure age for monazite in the pelitic gneiss. Also, garnets in these rocks show pronounced compositional zoning formed by diffusional modification during slow cooling. These results, combined with the absence of significant strain-related textures in either the nelsonite dike or the anatectic veins in the pelitic gneiss, demonstrates that Ottawan metamorphism in this region of the Adirondacks was dominantly a thermal, not a dynamic, event.

Even under such high grade conditions, the kinetics of mineral recrystallization were slow, contributing to the preservation of older assemblages. Recrystallization may have been inhibited by the dehydrated conditions that were the consequence of melt formation. This could explain the lack of younger generation, ca. 1020–1040 Ma zircon grains in the metapelites, although grains of this age are present in the nelsonite dike. Clarification of the conditions of Ottawan metamorphism in this region awaits further investigation.

Acknowledgements We thank Jim McLelland, Phil Whitney, Jeff Chiarenzelli, and Tony Philpotts for helpful discussions during this investigation. Special thanks go to Pat Bickford for his assistance with the zircon geochronology. John Valley and Jim McLelland made helpful comments on an earlier version of this paper, and constructive comments by L. Ron Frost and an anonymous reviewer on the penultimate manuscript are gratefully recognized. Support for this research included a Cortland College Faculty Research grant to RSD.

Appendix

Analytical techniques

Samples selected for U/Pb mineral geochronology were crushed by jaw mill and disc mill, then density separated with a Wilfly table. Further density separation was done using methylene iodide flotation. Heavy fractions obtained this way were then passed over a Frantz magnetic separator. Inclusion-free zircon and monazite fractions intended for analysis were hand picked. Selected grains were placed in screw-cap Teflon beakers and washed in warm distilled 7 M nitric acid for 20 minutes to several hours, followed by repeated cold nitric washes. Mineral grains were then pipetted into microcapsules, spiked with ca. 5° μg of mixed ^{205}Pb and ^{235}U tracer solution, and dissolved in HF at 240° C. This process was not uniformly effective for dissolving monazite grains, which in some cases required extra treatment with HCl or nitric acid.

After 35 to 40 hours, samples were decanted and dried. Samples were redissolved in 0.55 M column-cleaned HBr, then passed over Teflon microcolumns loaded with approximately 30 μl of cleaned Bio-Rad AG 1X8 anion resin. Uranium fractions were collected in the HBr washes and the lead fractions were then eluted in 6 M HCl. The same columns were rewashed and reequilibrated to 6 M HCl so that uranium fractions could be further purified after drying. Purified uranium was eluted with water. 2 μl of 0.25 N H_3PO_4 was added to both uranium and lead. Lead was loaded onto degassed Re filaments with 2 μl of silica gel. Uranium was loaded with an additional 2 μl of H_3PO_4 and approximately 0.5 μl of graphite so that they could be run as metal.

For every 13 samples, 2 total procedural blanks were created in parallel. Blanks were spiked after column chemistry and before drying down with approximately 1 ng of NBS983. Blanks ranged from 15 to 150 pg total lead.

All samples were run on a VG Sector multicollector mass spectrometer fitted with a Daly photomultiplier in the axial position. Correction for in-run fractionation using the Daly tube in multicollector mode was 0.1%/amu for all ratios except for $^{204}Pb/^{206}Pb$, which was 0.15%/amu.

The decay constants of Steiger and Jaeger (1977) were used in calculations. Isotopic data were reduced and upper intercept age determinations made using the reduction programs Pb-DAT and ISOPLOT (Ludwig 1980, 1989). Data are reported at the 2σ confidence level.

References

Berman RG (1990) Mixing properties of Ca-Mg-Fe-Mn garnets. Am Mineral 75: 328–344

Bohlen SR, Wall VJ, Boettcher AL (1983) Experimental investigations and geological applications of equilibria in the system FeO-TiO_2-Al_2O_3-SiO_2-H_2O. Am Mineral 68: 1049–1058

Bohlen SR, Valley JW, Essene EJ (1985) Metamorphism in the Adirondacks, I. Petrology, pressure, and temperature. J Petrol 26: 971–992

Bohlen SR, Dollase WA, Wall VJ (1986) Calibration and applications of spinel equilibria in the system FeO-Al_2O_3-SiO_2. J Petrol 27: 1143–1156

Buddington AF (1939) Adirondack igneous rocks and their metamorphism. Geol Soc Am Mem 7

Carl J, Sinha K (1992) Zircon U-Pb age of Popple Hill Gneiss and Hermon-type granite gneiss, NW Adirondack lowlands, NY. Geol Soc Am Abstr Prog 24: 11

Chakraborty S, Ganguly J (1992) Cation diffusion in aluminosilicate garnets: experimental determination in spessartine-almandine diffusion couples, evaluation of effective binary diffusion coefficients, and applications. Contrib Mineral Petrol 111: 74–86

Chiarenzelli JR, McLelland JM (1991) Age and regional relationships of granitoid rocks of the Adirondack highlands. J Geol 99: 571–590

Chiarenzelli JR, McLelland JM (1993) Granulite facies metamorphism, paleo-isotherms and disturbance of the U-Pb systematics of zircon in anorogenic plutonic rocks from the Adirondack Highlands. J Metamorphic Geol 11: 59–70

Clemens JD, Wall VJ (1981) Origin and crystallization of some peraluminous (S-type) granitic magmas. Can Mineral 19: 111–131

Copeland P, Parrish R, Harrison T (1988) Identification of inherited radiogenic Pb in monazite and its implications for U-Pb systematics. Nature 333: 760–763

Darling RS, Florence FP (1995) Apatite LREE chemistry of the Port Leyden Nelsonite, Adirondack Highlands, New York: implications for the origin of Nelsonite in anorthosite-surte rocks. Econ Geol (in press)

Edwards RL, Essene EJ (1988) Pressure, temperature and C-O-H fluid fugacities across the amphibolite-granulite transition, northwest Adirondack Mountains, New York. J Petrol 29: 39–72

Emslie R (1978) Anorthosite massifs, rapakivi granite, and the late Precambrian rifting of North America. Precambrian Res 7: 61–98

Epler NA (1987) Experimental study of Fe-Ti oxide ores from the Sybille Pit in the Laramie anorthosite, Wyoming. MSc dissertation, State University of New York at Stony Brook

Ganguly J, Saxena S (1984) Mixing properties of aluminosilicate garnets: constraints from natural and experimental data, and application to geothermo-barometry. Am Mineral 69: 88–97

Grove TL, Baker MB, Kinzler R (1984) Coupled CaAl-NaSi diffusion in plagioclase feldspar: experiments and applications to cooling rate speedometry. Geochim Cosmochim Acta 48: 2113–2121

Kolker A (1982) Mineralogy and geochemistry of Fe-Ti oxide and apatite (nelsonite) deposits and evaluation of the liquid immiscibility hypothesis. Econ Geol 77: 1146–1158

Koziol AM, Newton RC (1988) Redetermination of the anorthite breakdown reaction and improvement of the plagioclase-garnet-Al_2SiO_5-quartz geobarometer. Am Mineral 73: 216–223

Kretz R (1983) Symbols for rock-forming minerals. Am Mineral 68: 277–279

LaForce MJ, Darling RS, Hay RE (1994) Geophysical investigation of the Port Leyden nelsonite (abstract). Geol Soc Am Abstr Prog 26: 30

Lasaga AC (1983) Geospeedometry: an extension of geothermometry. In: Saxena SK (ed) Advances in physical geochemistry. Springer, New York, pp 81–114

Le Breton NC, Thompson AB (1988) Fluid-absent (dehydration) melting of biotite in metapelites in the early stages of crustal anatexis. Contrib Mineral Petrol 99: 226–237

Ludwig K (1980) Calculation of uncertainties of U-Pb isotopic data. Earth Planet Sci Lett 46: 212–220

Ludwig, K (1989) A plotting and regression program for radiogenic-isotopic data, for IBM-PC compatible computers, Version 1.05. US Geol Surv Open File Report 88–557

McLelland JM, Chiarenzelli J, Whitney P, Isachsen Y (1988a) U-Pb geochronology of the Adirondack Mountains and implications for their geologic evolution. Geology 16: 920–924

McLelland JM, Lochhead A, Vyhnal C (1988b) Evidence for multiple metamorphic events in the Adirondack Mountains, N.Y. J Geol 96: 279–298

McLelland JM, Daly SJ, Chiarenzelli J (1993) Sm-Nd and U-Pb isotopic evidence for juvenile crust in the Adirondack Lowlands and implications for the evolution of the Adirondack Mts. J Geol 101: 97–105

Mezger K, Rawnsley CM, Bohlen SR, Hanson GN (1991) U-Pb garnet, sphene, monazite, and rutile ages: implications for the duration of high-grade metamorphism and cooling histories, Adirondack Mts., New York. J Geol 99: 415–428

Mezger K, van der Pluijm BA, Essene EJ, Halliday AN (1992) The Carthage-Colton mylonite zone (Adirondack Mountains, New York): the site of a cryptic suture in the Grenville Orogen? J Geol 100: 630–638

Moore JM, Thompson P (1980) The Flinton group: a late Precambrian metasedimentary succession in the Grenville Province of eastern Ontario. Can J Earth Sci 17: 1685–1707

Newton RC, Haselton HT (1981) Thermodynamics of the garnet-plagioclase Al_2SiO_5-quartz geobarometer. In: Newton RC, Navrotsky A, Wood BJ (eds) Thermodynamics of minerals and melts. Springer, New York, pp 129–145

Nichols GT, Berry RF, Green DH (1992) Internally consistent gahnitic spinel-cordierite-garnet equilibria in the FMASHZn system: geothermobarometry and applications. Contrib Mineral Petrol 111: 362–377

Patino Douce AE, Johnson AD (1991) Phase equilibria and melt productivity in the pelitic system: implications for the origin of peraluminous granitoids and aluminous granulites. Contrib Mineral Petrol 107: 202–218

Parrish RR (1988) U-Pb systematics of monazite and its closure temperature based on natural examples. Geol Assoc Can Prog Abstr 13: 94

Philpotts AR (1967) Origin of certain iron-titanium oxide and apatite rocks. Econ Geol 62: 303–315

Powers RE, Bohlen SR (1985) The role of synmetamorphic igneous rocks in the metamorphism and partial melting of metasediments, NW Adirondacks. Contrib Mineral Petrol 90: 401–409

Spear FS, Florence FP (1992) Thermobarometry in granulites: pitfalls and new approaches. Precambrian Res 55: 209–241

Steiger RH, Jaeger E (1977) Subcommission on geochronology: convention on the use of decay constants in geo- and cosmochronology. Earth Planet Sci Lett 36: 359–362

Valley JW, O'Neil JR (1982) Oxygen isotope evidence for shallow emplacement of Adirondack anorthosite. Nature 300: 497–50

Valley JW, Bohlen SR, Essene EJ, Lamb W (1990) Metamorphism in the Adirondacks: II. The role of fluids. J Petrol 31: 555–596

Vielzeuf D, Holloway JR (1988) Experimental determination of the fluid-absent melting relations in pelitic system. Consequences for crustal differentiation. Contrib Mineral Petrol 98: 257–276

Watson EB, Harrison TM, Ryerson FJ (1985) Diffusion of Sm, Sr, and Pb in fluorapatite. Geochim Cosmochim Acta 49: 1813–1823

Wynne-Edwards HR (1972) The Grenville Province. In: Price RA, Douglas RJW (eds) Variations in tectonic styles in Canada. Geol Assoc Can Spec Pap 11: 263–334